Inversion of the diffraction pattern from an inhomogeneously strained crystal using an iterative algorithm

A. A. Minkevich,[1,*] M. Gailhanou,[1] J.-S. Micha,[2] B. Charlet,[3] V. Chamard,[1] and O. Thomas[1]
[1]*TECSEN, UMR CNRS 6122, Université Paul Cézanne, 13397 Marseille Cedex 20, France*
[2]*UMR SPrAM 5819, CEA-Département de Recherche Fondamentale sur la Matière Condensée, F-38054 Grenoble Cedex 9, France*
[3]*LETI, CEA Grenoble, 38054 Grenoble Cedex 9, France*
(Received 12 June 2007; published 17 September 2007)

The displacement field in highly nonuniformly strained crystals is obtained by addition of constraints to an iterative phase retrieval algorithm. These constraints include direct space density uniformity and also constraints to the sign and derivatives of the different components of the displacement field. This algorithm is applied to an experimental reciprocal space map measured using high-resolution x-ray diffraction from an array of silicon lines, and the obtained component of the displacement field is in very good agreement with the one calculated using a finite element model.

DOI: 10.1103/PhysRevB.76.104106 PACS number(s): 61.10.Nz, 42.30.Rx, 62.20.−x

I. INTRODUCTION

The need to understand the physical properties of micro- and nanocrystals leads to a fast development of techniques aimed at probing the local structure. In addition, small objects have much higher yield stresses as compared to their bulk counterparts,[1] and the vicinity of surfaces and interfaces implies strongly inhomogeneous stress fields. The experimental determination of the local strain remains, however, an open issue: Electron microscopy has the required spatial resolution but suffers from the need for sample thinning down to electron transparency, which modifies the strain field;[2] high-resolution x-ray diffraction is both strain sensitive and nondestructive, but, as the phase of the scattered field is not experimentally accessible, the strain profile at the nanometer scale is only achieved through a model dependent approach.[3,4] In this context, direct inversion based on x-ray diffraction is a rapidly progressing technique.[5–7] The possibility of directly determining the structure from a diffraction pattern alone was first mentioned by Sayre.[8] It is based on the "oversampling" conception, which allows us to recover all Fourier components of an object as soon as the diffracted intensity pattern is sampled with a rate σ at least twice the highest frequency, namely, the Nyquist frequency, which corresponds to the object size. The direct space electron density is retrieved with an iterative algorithm, first proposed by Gerchberg and Saxton[9] and further developed by Fienup,[10] relying on the fact that missing phases in most cases for two or more dimensional data can be uniquely recovered from the oversampled intensity information.[11] Since then, many versions of this algorithm were proposed as well as the comparisons of their convergence behavior properties.[12–14] The method is based on back and forth fast Fourier transforms (FTs) together with a set of constraints in both direct and reciprocal spaces. As it is based on FT, it is valid when the kinematical scattering at far field takes place. This approach has been very successful in yielding the density distribution of noncrystalline materials[5] and crystals.[15] The strain distribution is more difficult to retrieve since an effective complex-valued density is used, where the amplitude is the density of the unstrained crystal and the phase is approximately given by the scalar product of the displacement $\vec{u}$ with the reciprocal Bragg vector $\vec{G}_{hkl}$.[16] In this case, the convergence of the existing algorithms is often problematic and has hindered so far the general applicability of inversion to the diffraction of strained objects. For some special shapes, the convergence may be achieved.[17] The first success concerning the case of a weakly strained nanocrystal has been recently obtained,[6] but direct inversion of a diffraction pattern from a very nonuniformly strained crystal remains an unsettled problem.

In this paper, we present a method based on modifications of standard iterative algorithms, where additional constraints on the spatial phase variations and on the crystal density uniformity are introduced. The algorithm is successfully tested on experimental data, where the displacement field retrieved from the x-ray diffraction pattern measured on a highly nonuniformly strained crystal is in excellent agreement with the one calculated by finite element modeling based on continuum elasticity. The details of the developed iterative algorithm are explained in Sec. II. Section III contains the sample description and high-resolution diffraction experiment. Finally, the result of the inversion obtained with our algorithm is presented and discussed in the Sec. IV.

II. METHOD FOR STRAINED CRYSTAL DENSITY IMAGING

The error reduction[10] (ER) and the hybrid input-output[10,18] (HIO) iterative algorithms are standard inversion techniques used in the so-called lensless x-ray microscopy. They are iteratively and cyclically used together with a set of direct and reciprocal spaces constraints. At each algorithm iteration k, the difference between the calculated intensities and the experimental ones is expressed as

$$E_k^2 = \frac{\sum_{i=1}^{N} (|F_i^{calc}| - \sqrt{I_i^{meas}})^2}{\sum_{i=1}^{N} I_i^{meas}}, \quad (1)$$

where $|F_i^{calc}|$ is the magnitude of the calculated amplitude and I_i^{meas} is the measured intensity of point i in the reciprocal space map (RSM).

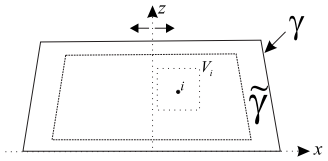

FIG. 1. Schematic sketch of the crystal cross section. V_i is the area around point i and $\tilde{\gamma}$ corresponds to a small region near support (γ) edges.

Unfortunately, in general, the application of this method is limited to the reconstruction a real positive valued function.[19] When the crystal is strained, its direct space density is not real and the positivity constraint cannot be applied. For a direct space complex-valued density, only the finite size support constraint defining the object size may be used. Very often, this constraint alone cannot provide reliable convergence of the method. The stagnation in iterative scheme appears without finding the correct solution. Such situation was observed for our case of inhomogeneously strained silicon on insulator line (see Sec. IV). Therefore, without additional *a priori* knowledge, the "phase problem" proved to be difficult to solve by this approach in the case of inhomogeneously strained crystals. In this context, the introduction of some additional constraints to the direct space is mandatory. The cost of these constraints has, however, to remain small; i.e., they should not require a fine preknowledge of the crystal to reconstruct. The approach presented in this paper is restricted to the case of two-dimensional (2D) plane strain systems and to chemically homogeneous crystals, although a generalization to three-dimensional (3D) systems might be foreseen. In order to lift the convergence problems, the following additional constraints in direct space were added.

(I) The density defined by direct space amplitudes must be uniform inside the support γ, except for a small region near the support edges $\tilde{\gamma}$, where it decreases in the external direction from the support (Fig. 1),

$$a_{k+1}(i) = \begin{cases} a'_k(i), & |a'_k(i) - c_k(i)| < \epsilon \\ a_k(i) + \beta[c_k(i) - a'_k(i)], & |a'_k(i) - c_k(i)| > \epsilon, \end{cases}$$

$$c_k(i) = \begin{cases} 0, & i \notin \gamma \\ \dfrac{\sum_{\tilde{i} \in V_i} a_k(\tilde{i})}{N_{V_i}}, & i \in \gamma \setminus \tilde{\gamma} \\ a'_k(i), & i \in \tilde{\gamma}, \end{cases} \tag{2}$$

with $a_k(i)$ is the amplitude of point i of input at the k iteration, $a'_k(i)$ is the amplitude of point i of output at the k iteration, the input $g_{k+1}(i) = a_{k+1}(i)e^{i\phi_{k+1}(i)}$ at the next iteration is taken from the output of the previous one by implementation of direct space constraints (for definitions of input and output, see Ref. 10), β is the parameter which is taken in the [0.5, 1.0] interval, ϵ is the parameter defining the threshold for applying the constraints (2) to each individual point i in the direct space map (DSM), V_i is the vicinity of point i defining the set of neighboring points around point i, N_{V_i} is the number of points in the V_i, $\tilde{\gamma}$ is the narrow edge of support, and the depth of this edge is defined by fittable parameters. The shape of V_i is not very important (disk, square, etc.). The number of points inside V_i should not, however, be too small. The amplitude profile inside the edge $\tilde{\gamma}$ is constructed automatically by the iterative algorithm.

It was found that only the constraint to amplitude uniformity is insufficient in providing convergence for the data presented in this paper. This constraint works (it was checked on modeled simulated data) only when the strain field inhomogeneity defined by the variation range of displacement field derivatives is small enough. When the amplitude of the derivative variation increases, this constraint alone does not allow us to find the solution anymore. For this reason, a second constraint was added.

(II) This second constraint is related to the maximum value that the components of the discrete displacement derivatives $\frac{\Delta_p u_j}{\Delta x_p}$ can take (Δx_p is a step along the p direction of the DSM, defining the spatial resolution in this direction). This maximum value limits the possible phase difference between neighboring points in the DSM,

$$|\phi_{k+1}(i) - \phi_{k+1}(i')| < G_{hkl}\Delta_p u_j^{max}, \tag{3}$$

where $\Delta_p u_j^{max}$ is a maximum difference in displacement component u_j between neighboring points i and i' along the p direction.

To make this constraint more efficient, it is necessary to define a minimum distance over which the displacement derivative $\frac{\Delta_p u_j}{\Delta x_p}$ sign is constant. These distances depend on the particular properties of the sample, such as shape, symmetry, origin of strain, etc., and they can be fitted during an iterative process.

To implement these constraints in the iterative algorithm, the maximum values of the displacement derivatives, namely, the magnitudes $\Delta_p u_j^{max}$, have to be estimated. It was found that for the iterative algorithm, a precise knowledge of the value of the maximum derivative is not very important. If condition (3) is satisfied for most of the object volume, the constraint to the phases [Eq. (3)] should be switched off at the last cycles of the iterative algorithm. Alternatively, instead of an estimation of the value of $\Delta_p u_j^{max}$, a trial-and-error procedure can be easily performed.

III. EXPERIMENT

Here, we describe high-resolution diffraction measurements in the vicinity of 004 Bragg reflection from Si lines on SiO_2/Si substrate.[20] The Si lines were obtained by etching through a 160 nm thick Si_3N_4 mask a blanket 100 nm silicon on insulator (SOI) film which lies on the top of a 200 nm buried oxide layer [Fig. 2(b)]. The direction of the lines is parallel to the [010] direction of the SOI crystal and to the [110] direction of the substrate crystal. The system is chemically homogeneous and uniform in the direction of the lines, and the strain field is therefore essentially 2D. The 2D high-resolution diffraction pattern was measured on the French CRG beamline BM32 at ESRF around the 004 Bragg reflection [Fig. 2(a)] in the plane (x,z) normal to the sample sur-

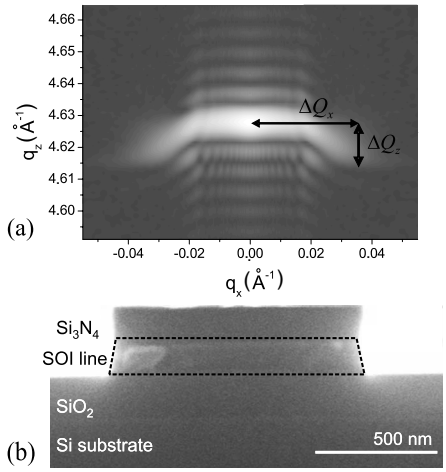

FIG. 2. (a) RSM measured near 004 reflection from Si lines on SiO_2/Si substrate. The intensity scale is logarithmic. (b) Scanning electron microscopy image of the cross section of the corresponding sample. The investigated Si on insulator (SOI) line is emphasized by a dotted line contour for sake of clarity.

face and to the SOI lines ($x \| q_x \|$SOI [100] direction, $z \| q_z \|$SOI [001] direction, and $y \|$SOI line). Here, q_x and q_z are the components of $\vec{q}=\vec{k}_f-\vec{k}_i$, $|\vec{k}_f|=|\vec{k}_i|=\frac{2\pi}{\lambda}$, $\vec{k}_i$ and $\vec{k}_f$ are the incident and diffracted wave vectors, respectively. The wavelength $\lambda=1.54$ Å was selected using a Si (111) monochromator. The SOI sample was mounted at the center of a (2+2) circle diffractometer with a triple-bounce Si (111) analyzer and a NaI:Tl scintillator. The beam size at the sample position was 500×500 μm^2. The [001] directions of both crystals are misaligned by 0.4°. This small off orientation enables the measurement of the diffraction pattern of SOI lines in the vicinity of $\vec{G}_{004}$ Bragg vector without any overlap from the intensity scattered from the substrate. It is important to note in Fig. 2(a) the absence of periodic truncation rods expected from the interferences between lines in spite of an x-ray coherence in this direction length of around 6 μm, which is much larger than the 2 μm line period. This is due to important random phase shifts between lines, which might be related to very small (1 Å range)—but comparable to the inverse of the scattering vector—ripples at the SiO_2 surface.[21] Since a lot of perfectly uniform lines are illuminated by the incident beam with a coherence length much larger than the linewidth, the measured 2D diffraction pattern is equivalent to the diffraction pattern of a single SOI line. In the case of the 004 Bragg reflection, the measured diffraction pattern contains only the information on the u_z component of the displacement field $\vec{u}$. In order to be able to apply the iterative inversion algorithm to the measured intensity, it is necessary to satisfy the oversampling condition $\sigma_{x,z}=\frac{M_{x,z}}{L_{x,z}}>2$ in the DSM by choosing the appropriate step $\Delta q_{x,z}=\frac{2\pi}{M_{x,z}}$ in the RSM, where $M_{x,z}$ is the size of the DSM and $L_{x,z}$ is the expected size of the object (support) in the corresponding dimension x or z. It has been shown[22] that it is unnecessary to have an oversampling ratio $\sigma>2$ in each

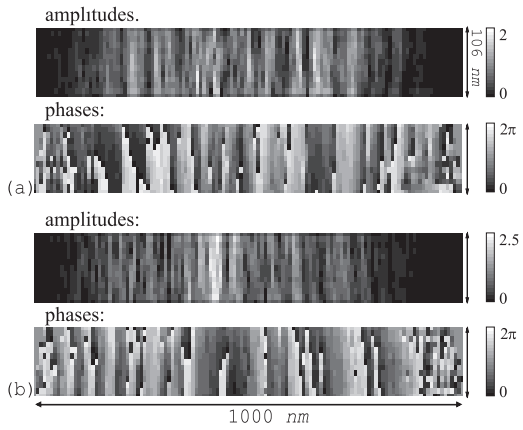

FIG. 3. [(a) and (b)] Two typical solutions of the inverse problem using standard algorithms (ER+HIO): Amplitudes (in arbitrary units), corresponding to the shape and density of SOI line, and phases (in radians).

dimension to retrieve 2D and 3D objects. However, practically for more reliable reconstructions, it is better to have both $\sigma_{x,z}\gg2$. In our experiment, the oversampling ratio was chosen to be $\sigma_z\approx7.8$ and is related to the number of measured points per thickness oscillation along q_z in the RSM. In the x direction, the experimentally chosen step Δq_x corresponds to an oversampling ratio $\sigma_x\approx6.3$. The steps $\Delta x\approx7.9$ nm and $\Delta z\approx8.4$ nm in the DSM define the attainable resolution and relate to the size of the RSM. The size of the RSM is restricted by the area where the signal is above the background.

IV. STRAIN FIELD RECONSTRUCTION: RESULTS AND ANALYSIS

The data in Fig. 2(a) were analyzed using the iterative phase retrieval algorithm. For each time, the algorithm was applied with a new set of random phases in RSM. Two typical results from the standard algorithm with support constraint, which exactly correspond to the shape of SOI line, are shown in Fig. 3. Both amplitudes and phases represent modulated profiles with random behavior, which do not have any physical meaning. Moreover, the results are not consistent from one pass of algorithm to another. However, the error metrics is very small and varies in the interval $E_k^2\sim[1.7\times10^{-3},2\times10^{-3}]$. It means that, in the case of an inhomogeneously strained crystal expressed as a complex-valued density, different combinations of amplitudes and phases in direct space can yield very similar FT amplitude images. They correspond to local minima with very small error metric (1) causing the appearance of an ambiguity in the solutions. This is especially the case for experimental data where, because of the presence of noise, the difference between error metrics of correct and local minima solutions vanishes. Once the algorithm reached the local minima with such a small error metric, it stagnates near it, i.e., further iterations do not produce any significant changes. In this case, the zero density region outside the support, arising from signal oversampling, cannot compensate for the un-

known phases in the diffraction pattern, because the values in this area become negligibly small.

Experimental artifacts are not a reason for the nonconvergence, as a study was also done on noise-free modeled simulated data leading to the same conclusion. This is a mathematical problem of convergence of iterative algorithms in the case of complex-valued objects. It is also interesting to point out that when the values of deformations were artificially reduced to the values similar to those reconstructed in Ref. 6, the solution was found by standard methods. This clearly shows that standard iterative algorithms are not effective for the case of highly inhomogeneously strained crystals.

We now describe the application of the previously described modified algorithm to the same experimental data. The direct space constraints, discussed in the first part of this paper, were added to the iterative phase retrieval algorithm in addition to the standard support constraint. Supplementary to these direct space constraints, the symmetry property of the displacement field with respect to the vertical axis z shown on Fig. 1 was used. An estimation of the maximum values of the displacement derivatives $\frac{\Delta_x u_z^{\max}}{\Delta x}$ and $\frac{\Delta_z u_z^{\max}}{\Delta z}$ (Δx and Δz are steps along x and z of the DSM, respectively) was also carried out from experimental data. The corresponding magnitude of the derivative of u_z along x is found from the distance ΔQ_x [shown on Fig. 2(a)] via the relation $\Delta Q_x = G_{004} \frac{\Delta_x u_z^{\max}}{\Delta x}$. This value corresponds to a $\frac{3}{4}\pi$ maximum phase difference in the DSM between neighboring points along x. Similarly, the magnitude for the maximum displacement derivative u_z along z, $\frac{\Delta_z u_z^{\max}}{\Delta z}$, is calculated from the distance ΔQ_z [shown on Fig. 2(a)] via the relation $\Delta Q_z = G_{004} \frac{\Delta_z u_z^{\max}}{\Delta z}$. The validity of these estimations was checked at the end of the inversion.

A good starting point for the shape was obtained from measurements on the scanning electron micrograph. The thickness oscillations along the z direction, which are clearly observed in the RSM because of the small strain gradient in this direction, also provided a good estimation. The adaptive shrink-wrap procedure,[23] which starts from a larger support and gradually removes from it the pixels whose amplitudes tend toward zero, does not work in our case. For this reason, a support fitting procedure was developed in order to gradually change the support area γ and the edge of the support $\tilde{\gamma}$ during the iterations. Generally, one cycle of iterative algorithm included consecutively 50 iterations of ER, 50 iterations of HIO, 50 iterations of modified HIO [Eq. (2)] with phase constraints [Eq. (3)], and 50 iterations of modified HIO (only constraints to amplitudes [Eq. (2)]). If the support is very well defined (i.e., it corresponds to the exact shape of the object), the finding of the solution takes about four to eight cycles. Many trials of the algorithm were performed starting from random phases in RSM and each time converged to the solution with $E_k^2 \approx 10^{-3}$. With respect to the accuracy of the data, all the solutions are the same, and one of them is plotted in Fig. 4. The discontinuities in the retrieved phases map are related to the crossing of phases through 2π (2π corresponds to a displacement equal to $\frac{2\pi}{G_{004}}$). Some strain ϵ_{zz} along z is also found gradually appearing at the edges of the line, in the region where the derivative $\frac{\partial u_z}{\partial x}$ becomes very high. This strain causes the appearance of the

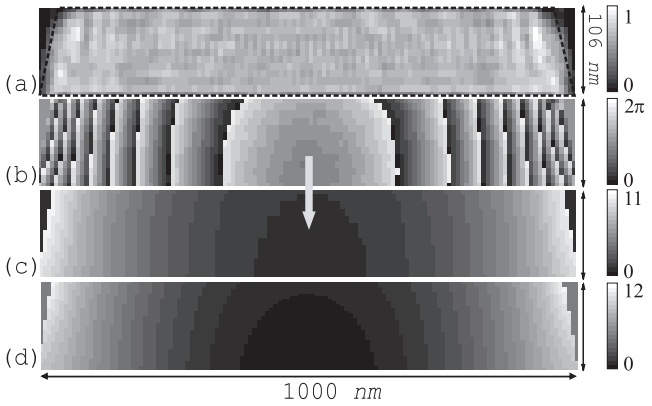

FIG. 4. The solution of the inverse problem: (a) Amplitudes (in arbitrary units), which represent shape and density of SOI line [the dotted line trapezoid corresponds to the trapezoid of Fig. 2(b)], (b) phases (in radians), (c) retrieved displacement field u_z (in Å), and (d) displacement field u_z, calculated by finite element modeling (in Å) (Ref. 20).

"moustache" shape intensity distribution in the RSM. There is also a small amount of homogeneous strain in the z direction, which was found from the difference in q between the Bragg maxima of SOI lines and Si substrate. Using the retrieved phases, the displacement field was calculated [Fig. 4(c)]. The maximum value of the displacement u_z is about 11 Å.

The main advantage of this approach is its model independence as opposed to the case of, for example, finite element calculations. Such calculations were also done for this sample, considering the residual stress in the Si_3N_4 top layer as the reason for the strain appearance in the line.[20] The displacement fields obtained by these two approaches are in very good agreement [Figs. 4(c) and 4(d)], which definitely validates our inversion procedure.

V. CONCLUSION

We have presented a modified iterative algorithm with additional direct space constraints. It is shown that the displacement field in a highly inhomogeneously strained crystal can be retrieved from its x-ray diffraction pattern alone. This algorithm is applied to retrieve the displacement field inside SOI lines from experimental data. In this particular case, finite element modeling was also possible and quite successful in describing the displacement field, and a very good agreement between the two methods was found. This opens important perspectives for local strain determination at the nanoscale, in particular, for the cases where the model dependent approach cannot be used.

ACKNOWLEDGMENTS

A.A.M. is very grateful to S. Labat for discussions. The ESRF is acknowledged for beam time allocation.

*andrey.minkevich@univ-cezanne.fr

[1] E. Arzt, G. Dehm, P. Gumbsch, O. Kraft, and D. Weiss, Prog. Mater. Sci. **46**, 283 (2001).
[2] M. M. J. Treacy, J. M. Gibson, and A. Howie, Philos. Mag. A **51**, 389 (1985).
[3] T. Baumbach, D. Luebbert, and M. Gailhanou, J. Phys. D **32**, A208 (1999).
[4] Q. Shen and S. Kycia, Phys. Rev. B **55**, 15791 (1997).
[5] J. Miao, P. Charalambous, J. Kirz, and D. Sayre, Nature (London) **400**, 342 (1999).
[6] M. A. Pfeifer, G. J. Williams, I. A. Vartanyants, R. Harder, and I. K. Robinson, Nature (London) **442**, 63 (2006).
[7] A. Y. Nikulin, Phys. Rev. B **57**, 11178 (1998).
[8] D. Sayre, Acta Crystallogr. **5**, 843 (1952).
[9] R. W. Gerchberg and W. O. Saxton, Optik (Stuttgart) **35**, 237 (1972).
[10] J. R. Fienup, Appl. Opt. **21**, 2758 (1982).
[11] R. H. T. Bates, Optik (Jena) **61**, 247 (1982).
[12] V. Elser, J. Opt. Soc. Am. A **20**, 40 (2003).
[13] H. H. Bauschke, P. L. Combettes, and D. R. Luke, J. Opt. Soc. Am. A **19**, 1334 (2002).
[14] S. Marchesini, Rev. Sci. Instrum. **78**, 011301 (2007).
[15] G. J. Williams, M. A. Pfeifer, I. A. Vartanyants, and I. K. Robinson, Phys. Rev. B **73**, 094112 (2006).
[16] S. Takagi, J. Phys. Soc. Jpn. **26**, 1239 (1969).
[17] J. R. Fienup, J. Opt. Soc. Am. A **4**, 118 (1987).
[18] R. P. Millane and W. J. Stroud, J. Opt. Soc. Am. A **14**, 568 (1997).
[19] J. R. Fienup and A. M. Kowalczyk, J. Opt. Soc. Am. A **7**, 450 (1990).
[20] M. Gailhanou, A. Loubens, J.-S. Micha, B. Charlet, A. A. Minkevich, R. Fortunier, and O. Thomas, Appl. Phys. Lett. **90**, 111914 (2007).
[21] J. Härtwig, S. Köhler, W. Ludwig, H. Moriceau, M. Ohler, and E. Prieur, Cryst. Res. Technol. **37**, 705 (2002).
[22] J. Miao, D. Sayre, and H. N. Chapman, J. Opt. Soc. Am. A **15**, 1662 (1998).
[23] S. Marchesini, H. He, H. N. Chapman, S. P. Hau-Riege, A. Noy, M. R. Howells, U. Weierstall, and J. C. H. Spence, Phys. Rev. B **68**, 140101(R) (2003).